COBEM 2021 26th International Congress of Mechanical Engineering
November 22-26, 2021, Virtual Congress, Brazil
ABCM Associação Brasileira de Engenharia e Ciências Mecânicas

COB-2021-0943
EVALUATION OF CIRCULARITY MEASUREMENT THROUGH LIMAÇON APPROXIMATION AND A LIGHT DETECTION AND RANGING (LiDAR) SYSTEM

Vinícius Conti da Costa
Bruno Ziegler Haselein
Filipe Barbosa Veras
Manoel Kolling Dutra
Tiago Loureiro Figaro da Costa Pinto
Federal University of Santa Catarina, Department of Mechanical Engineering, Florianópolis, SC, Brazil
vinicius.costa@labmetro.ufsc.br
haselein.bruno@gmail.com
filipe.veras@labmetro.ufsc.br
manoel.kolling@posgrad.ufsc.br
tiago.pinto@ufsc.br

Abstract. *Pipelines are an important part in systems for production, transportation and consumption in the oil and gas industries. As the main objects of pipeline transport systems, pipes are subject to strict requirements for the quality of the manufacturing materials, production technology, coating quality, as well as their geometric and dimensional aspects. In order to provide inspection of pipes at all stages of logistical movement, it is necessary to find a measurement method that can quickly measure the inner pipe diameter and geometry in complex environments. However, it is not practical to align a rotary axis measurement system (MS) on the longitudinal axis of a cylindrical pipe with good accuracy, and subsequent measurements will not directly provide geometric errors, as circularity. So, if there is a small eccentricity in the MS positioning, the inner circle that this instrument aims to measure can be approximated by a geometry called limaçon. This approach results in a linear equation to identify the unknown measurement parameters, making trivial the process of determining the center and radius of the measurand. This study presents the evaluation of an active measurement system called Light Detection and Ranging (LiDAR) with a 360° rotation axis as MS and uses limaçon approximation to calculate the decentralization of the MS and the circularity error of the measurand. The experimental procedure includes positioning the LiDAR on a plane perpendicular to the axial axis of the measurand and capturing data in four positions, i.e., one with the MS approximately concentric to the measurand, and the others with offsets. In the sequence, the calculation of the circularity deviation by limaçon approximation and uncertainty measurement are performed to evaluate sources of uncertainty, such as resolution and Azimuth angle. In addition, the effect of several parameters, such as angular rate, angular speed and number of revolutions are evaluated, and the results are compared with those obtained through an articulated 3D measuring arm. The results indicate that the smallest circularity error occurs when the LiDAR is near to the center and the error due to the approximation in limaçon tends to zero when there is no eccentricity. However, the proposed approach is not suitable for large eccentricities. In addition, the lower the angular velocity of the LiDAR, the greater the measurement error due to a bigger point cloud measured in a single revolution when at low speed, which results in more surface details.*

Keywords: *Pipe inspection, Circularity Measurement, Limaçon Approximation, LiDAR.*

1. INTRODUCTION

Pipelines are widely used in oil, gas and petrochemical industries to transfer different fluids between oil platforms, refineries and petrochemical plants (Adegboye *et al.*, 2019). As the main objects of pipeline transport systems, pipes are subject to strict requirements for the quality of the manufacturing materials, production technology, coating quality, as well as their geometric and dimensional aspects (Hredil *et al.*, 2019). In order to provide inspection of pipes at all stages of logistical movement, it is necessary to find a measurement method that can quickly measure the inner pipe diameter and geometry in complex environments.

Computer vision techniques for 2D/3D measurement have been constantly applied in industry due to its touchless data acquisition nature and fast quantitative results. In this context, laser triangulation, as exemplified in (Figure 1a), is an optical method that only require a laser source and an optical sensor or camera (Sun *et al.*, 2015). The method projects

the structured light to an object, while a camera/sensor captures the feedback of the laser and uses this information to determine distance from an object (Figure 1b).

(a) Laser triangulation method (Movimed, 2018). (b) RPLiDAR scanning illustration (Slamtec, 2017).

Figure 1: Laser triangulation illustration.

Light Detection and Ranging (LiDAR) scanners are based on laser triangulation and appropriate to measure the internal geometry of a pipe section in industrial environments due to its fast processing time and 360 degrees data acquisition. These systems work with one or more laser pointers, which are normally infrared and do not interfere with other sensors (cameras, optical sensors, human eye).

Due to the impracticality of positioning a measurement system (MS) precisely centered on a cylinder, mathematical methods, e.g., Gauss–Newton (Muralikrishnan and Raja, 2008), are commonly applied to estimate the unknown parameters of the measurand, e.g., maximum and minimum radius. These methods, however, usually rely on iterative calculations which, according to the method, may result in undesirable outcomes, such as local optimum or excessive computational time.

In this paper, we propose to evaluate the use a LiDAR system and a non-iterative parameter estimation method, in which the inner circle of a cylinder is approximated by a geometry called limaçon (Eves, 1965), to verify the circularity of a pipe. In this method, a non-concentric position of the MS will result in a measurement error called "limaçon effect", where the results of the scan will be similar to a limaçon-shaped geometry (Figure 2), instead of a circle (Samuel and Shunmugam, 2003). Due to the aforementioned reasons, we conducted and analysed several experiments on the use of a LiDAR system and limaçon approximation to estimate the unknown parameters of a pipe. Furthermore, we compared our results with the ones obtained with a 7-axis coordinate measuring machine (CMM) and with the Gausian best-fit method.

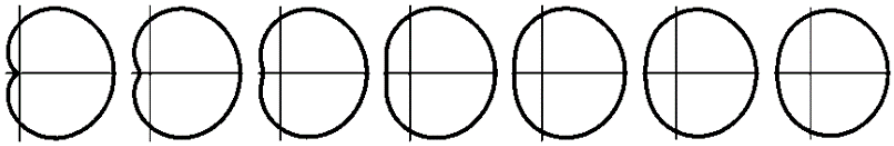

Figure 2: Limaçon shapes (Anton *et al.*, 2014).

The paper is organized as follows. This first section briefly presents the motivations for using LiDAR system and limaçon approximation to measure circularity. In section 2, the sources of uncertainty on circularity measurement are discussed, as well as the application of the limaçon approximation to estimate the center of the circle and how to correct it to maintain measurand and measurement system mathematically concentric. The equipments and methodology are explained in section 3, followed by the results and evaluation of the technique in section 4. Finally, section 5 summarizes the lessons learned.

2. CIRCULARITY MEASUREMENT

Circularity verification is a process commonly performed in production lines. In order to do so, the circularity deviation is determined in a circular section of a cylindrical element and is defined by the minimum radial distance between two concentric circumferences, called minimum zone reference circles, which the measurand need to be contained (Souza *et al.*, 2012), as well as represented in Figure 3, where MMZRC is the Mean Minimum Zone Reference Circle, OMZRC is the Outer Minimum Zone Reference Circle and IMZRC is the Inner Minimum Zone Reference Circle.

According to (Poldrack, 2019) and (Souza *et al.*, 2012), the cross section where roundness is evaluated has its analysis divided in two major groups: continuous measurements, with infinite points to define the geometry; and discrete measurements, considering a determined number of points to define the shape. However, regardless the selected system, concentricity is a major topic that must be addressed.

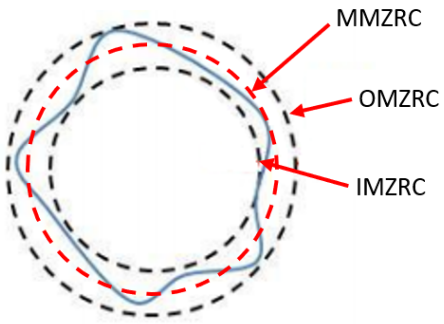

Figure 3: Graphic representation of circularity. (Souza *et al.*, 2012)

When mounting a part on a rotary measurement system, it is not practical to center the part precisely and, due to this eccentricity, subsequent measurements do not directly provide geometric errors, as circularity. To cope with this issue, best-fit techniques, which are based on Cartesian coordinates and involve iterative calculations, are commonly employed. In this context, several algorithms, such as steepest descent, Gauss–Newton and Levenberg–Marquardt, are used to identify the unknown parameters in non-linear Least-Squares (LS) circle fitting techniques (Muralikrishnan and Raja, 2008). However, although these techniques are commonly used in industrial applications, several issues have to be addressed in order to achieve satisfactory accuracy in the measurements, such as computational calculation time, local minimum and maximum, and parameters optimization.

In contrast to best-fitting approaches, Chetwynd (1979) and Chetwynd and Phillipson (1980) proposed to approximate the circle by a geometry called limaçon (Eves, 1965) and using polar coordinates, therefore avoiding iterations and allowing the direct definition of the unknown parameters, i.e., eccentricity and radius. However, as further discussed in section 4, the quality of this approximation depends on the eccentricity, that is, the farther from the center the MS is, the bigger is the circularity error after limaçon approximation correction.

2.1 Limaçon approximation

In this section, we present the mathematical background necessary to comprehend the experiments detailed in section 3.2. First, in order to facilitate the limaçon approximation parameters representation, Figure 4 presents the probe as a moving object around a circular part of radius r and eccentricity (a, b) on two orthogonal axes.

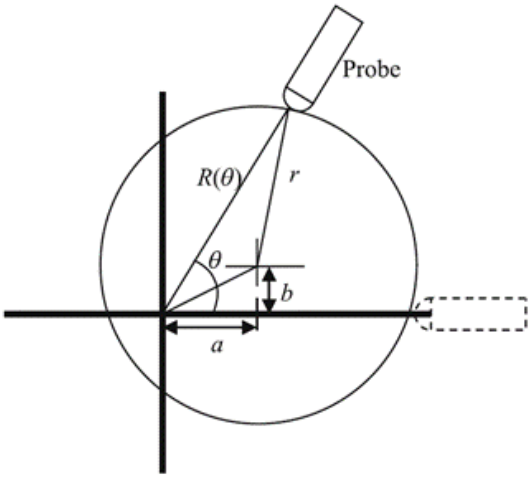

Figure 4: Limaçon approximation parameters (Muralikrishnan and Raja, 2008).

Accordingly, the radial deviation $R(\theta)$ is defined as a function of angle θ through Eq. (1)

$$R(\theta) = a\cos\theta + b\cos\theta + \sqrt{r^2 - (a^2+b^2)\sin(\theta-\phi)} = a\cos\theta + b\cos\theta + r\sqrt{1 - \frac{(a^2+b^2)\sin(\theta-\phi)}{r^2}}, \quad (1)$$

where

$$\phi = \tan^{-1}(b/a)$$

In cases of small eccentricity, $R(\theta)$ can be approximated as

$$R(\theta) \approx a\cos\theta + b\cos\theta + r \tag{2}$$

If there are n measurement points, Eq. (2) can be written in matrix form $AP = B$, where

$$A = \begin{bmatrix} \cos\theta(1) & \sin\theta(1) & 1 \\ ... & ... & ... \\ \cos\theta(n) & \sin\theta(n) & 1 \end{bmatrix}, P = \begin{bmatrix} a \\ b \\ r \end{bmatrix}, B = \begin{bmatrix} R(1) \\ ... \\ R(n) \end{bmatrix} \tag{3}$$

As demonstrated by (Muralikrishnan and Raja, 2008), if the data points are uniformly distributed on the circumference, the LC center and radius are obtained directly through Eqs. (4, 5 and 6), respectively:

$$a = (2/n)\sum_{i=1}^{n}\cos\theta(i)R(i) \tag{4}$$

$$b = (2/n)\sum_{i=1}^{n}\sin\theta(i)R(i) \tag{5}$$

$$r = (1/n)\sum_{i=1}^{n}R(i) \tag{6}$$

Finally, the error due to the limaçon approximation is calculated through Eq. (7):

$$\varepsilon = \sqrt{r^2 - Ecc^2\sin(\theta - \phi)} - r \tag{7}$$

where

$$Ecc = \sqrt{a^2 + b^2}$$

3. MATERIALS AND METHODS

This paper is based on an experimental procedure which includes positioning a LiDAR on a plane perpendicular to the axial axis of the measurand and capturing data in four positions, i.e., one with the measurement system approximately concentric to the measurand, and the others with offsets. As an environment standard it was induced a thermal stability between measurand, measurement system and measurement environment, letting the components in controlled temperature of $20°C$ during 72 hours. In the sequence, the calculation of the circularity deviation by limaçon approximation and uncertainty measurement are performed to assess sources of uncertainty, such as resolution and Azimuth angle. In addition, the effect of several parameters, namely angular rate, angular speed and number of revolutions, are evaluated. Finally, the results are compared with those obtained through an articulated 3D measuring arm.

3.1 Reference system: Articulated 3D Measuring Arm

A 7-axis coordinate measuring machine (CMM), articulated arm Faro Edge and Faro Laser ScanArm Edge with a spherical working volume was selected as the reference system. In this system, each joint has a rotary optical encoder, and the signals from these encoders are processed using advanced error coding and temperature compensation technology (Faro, 2016). For this test, the following 3-steps experimental procedure using the CMM was applied:

1. Perform circularity measurements on a section perpendicular to the axial axis (y) of the measuran, i.e., to obtain 30 points to each one of the 5 circularity measurement sets;
2. Calculate circularity via software FARO CAM2;
3. Calculate the extended uncertainty.

In order to complement the aforementioned experimental procedure, Figure 5 shows the measurement with the articulated 3D measuring arm.

As detailed in Table (1), the extended uncertainty of the articulated 3D measuring arm measurements computes the following sources of uncertainty: repeatability, MS resolution, 2RMS and mechanical probe. In this table, standard uncertainty (mm) and degrees of freedom are represented by the terms "u" and "v", respectively. Accordingly, the circularity error obtained in this experiment was $0.889 \pm 0.078mm$.

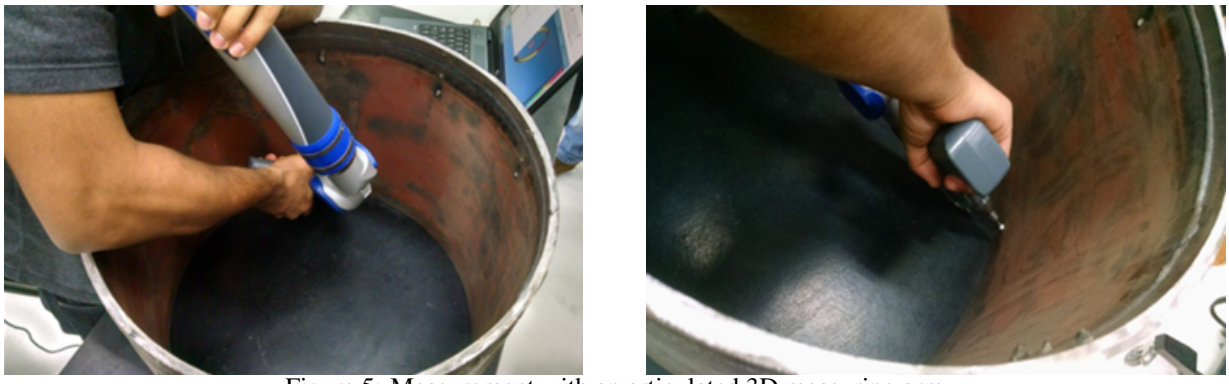

Figure 5: Measurement with an articulated 3D measuring arm.

Table 1: Extended uncertainty on the articulated 3D measuring arm measurements

Measurement Process:		Articulated 3D measuring arm			Unit:	mm
Sources of uncertainty		Systematic effect	Aleatory effects			
Symbol	Description	Correction	a	Distribution	u	v
Rep	Repeatability	-	-	Normal	0.027	4
Res	MS resolution	-	$5E-05$	Rectangular	$2.89E-05$	∞
$u.SM$	2RMS	-	0.034	Rectangular	0.019	∞
$u.A$	Mechanical probe	-	0.012	Rectangular	0.007	∞
c_c	Combined correction	-				
u_c	Combined uncertainty			Normal	0.034	10
U	Expanded uncertainty			Normal	0.078	
$RM = (0.889 \pm 0.078)mm$						

3.2 Light Detection and Ranging (LiDAR) System

In our experimental procedure, a Laser-based triangulation sensor RPLiDAR A2M8 was used. The system consist of range scanner constantly rotating 360° clockwise from an motor attached through a belt providing range scan data within 8 meters of its range. Furthermore, the RPLIDAR A2M8 has a speed adaptive system where the frequency of the laser scanner automatically changes according to the motor speed. The system, which able to work in indoor as well as outdoor environments without sunlight, emits modulated infrared signal and then the returning signal is detected and sampled by a vision acquisition module. Finally, a digital signal-processing module processes the sampled data and outputs the distance and the angle between the object and the LiDAR (Slamtec, 2017).

Table (2) summarizes relevant characteristics of the SLAMTEC RPLIDAR A2M8 employed. In this table, it is important to differentiate frequency, i.e., the number of points obtained per second, from scan rate, i.e., the number of revolutions per second.

Table 2: Characteristics of SLAMTEC RPLIDAR A2M8

Item	**Unit**	**Min.**	**Typical**	**Max.**	**Observation**
Distance	m	0.15	-	8	70% of reflection
Angle	degrees	-	$0-360$	-	-
Scan	degrees	-1.5	-	1.5	-
Distance Resolution	mm	-	< 0.5	-	$< 1.5m$
			$< 1\%$ of distance		Other distances
Angular Resolution	degrees	0.45	0.9	1.35	To Scan Rate $= 10Hz$
Pulse Width	ms	-	0.125	-	-
Frequency	Hertz	2000	4000	4100	-
Scan Rate	Hertz	5	10	15	$400ppr$ for typical

In order to evaluate the applicability of a LiDAR as MS and limaçon approximation to calculate the decentralization of the MS and the circularity error of the measurand, the following steps were followed:

1. Position the LiDAR on a plane perpendicular to the axial axis (y) of the measurand. In order to do so, we placed the machined surface of the cylinder on a metrological bench, and the LiDAR inside the cylinder (Figure 6);

2. Capture data in four positions, i.e., one with the MS approximately concentric to the measurand ($r = 0.558 \pm 0.001\,mm$), and the others with offsets ($r = 27.795 \pm 3.729\,mm, 57.347 \pm 7.962\,mm$, and $85.755 \pm 20.896\,mm$), respectively, at angular velocity $11.3Hz$. It is important to mention that in this last test we chose to position the MS at a distance below the minimum allowed according to the equipment specifications to evaluate its behavior in this scenario.
3. Capture data with the MS approximately concentric in three angular velocities: $5.7\ Hz$, $11.3\ Hz$ and $14.9\ Hz$;
4. Use limaçon approximation to identify the unknown parameters, i.e., LC center and radius;
5. Calculate circularity;
6. Calculate the expanded uncertainty;
7. Compare the results with those obtained with the articulated 3D measuring arm.

Figure 6a represents the simulated experiment which was used to define work parameters, and Figure 6b the real experiment, representing the measurement process using LiDAR. In section 4, the results are presented, and the circularity error and the expected circularity with the limaçon approximation discussed.

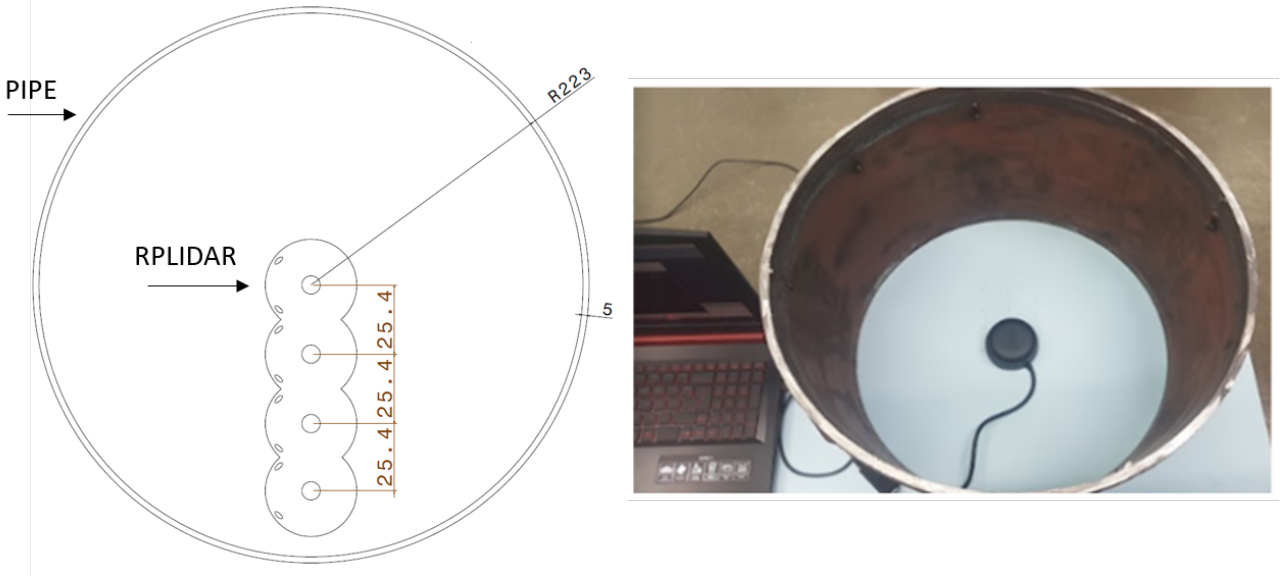

(a) Simulated experiment

(b) Real experiment

Figure 6: Representations of experiment using LiDAR.

4. RESULTS AND DISCUSSION

In this section, the results obtained are presented and critically discussed. First, based on the R^2 shown in Figure 7, it is reasonable to assume the angle θ presents a linear increment in the two evaluated point densities, that is, a point cloud with 362 and a point five times denser, with 1806 data points. As previously mentioned, if the data points are uniformly distributed on the circumference, the LC center and radius are obtained directly through Eqs. (4, 5 and 6).

Below, in Table (3), it's possible to analyze the first steps of the roundness uncertainty evaluation, where were defined the circularity error, the eccentricity, the limaçon error, and the maximum and minimum radius R_{min} and R_{max}. The data exposed in Table (3) was synthesized, and can be consulted entirely in (Costa *et al.*, 2021).

Based on Table (3) and Norm JCGM 100:2008, Table (4) presents the default process to find the uncertainty associated with circularity deviations. It is worth mentioning that the azimuth angle is not presented in this table because the error from this source of uncertainty is negligible in our experiments (Costa *et al.*, 2021). Similarly, the content in Table (5) summarizes the process presented in Table (4) applied to the proposed experiments.

The Figure 8 shows some results related to the limaçon approximation. In Figure 8a, the measurement system is highly concentric with the measurand and the roundness error is totally defined by OMZRC and IMZRC, and when the results are amplified, the digital increment nature of A2M8 LiDAR is evidenced. In Figure 8b, due to eccentricity of $85,755\ mm$, a limaçon-shaped geometry generated through the limaçon approximation is represented in red, while the blue line represents the point cloud obtained in this experiment.

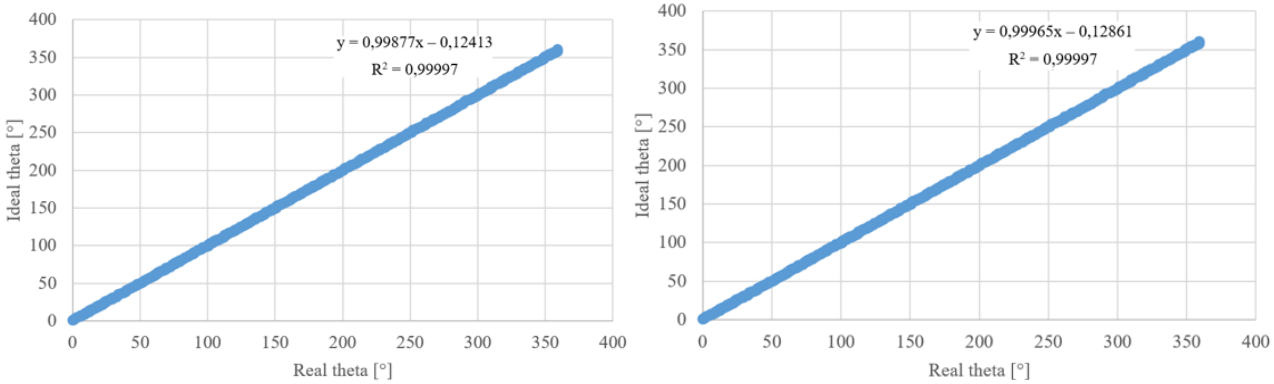

(a) θ with 362 data points.

(b) θ with 1806 data points.

Figure 7: Linear regression of θ with 362 and 1806 data points, respectively.

Table 3: Means and standard deviations of the experiments.

Experiment 01			**Experiment 02**		
	mean (mm)	stddev (mm)		mean (mm)	stddev (mm)
Circularity error	2.707	0.295	Circularity error	3.730	0.058
Eccentricity	0.558	0.022	Eccentricity	27.795	0.011
Limaçon error	0.001	$5.658E-5$	Limaçon error	1.732	0.002
R_{min}	221.950	0.318	R_{min}	220.168	0.196
R_{max}	224.657	0.067	R_{max}	223.897	0.197
Experiment 03			**Experiment 04**		
	mean (mm)	stddev (mm)		mean (mm)	stddev (mm)
Circularity error	7.962	0.332	Circularity error	20.896	0.103
Eccentricity	57.347	0.046	Eccentricity	85.755	0.022
Limaçon error	7.411	0.014	Limaçon error	16.641	0.004
R_{min}	214.380	0.220	R_{min}	202.867	0.093
R_{max}	222.3422	0.187	R_{max}	223.763	0.033

Table 4: Uncertainty associated with circularity deviation measurements using A2M8 in position 1.

Measurement process:		Circular error position 1 A2M8			Unit:	mm
Sources of uncertainty		Systematic effects	Aleatory effects			
Symbol	Description	Correction	a	Probability Distribution	u	v
Rep	Repeatibility	-	-	Normal	0.132	4
Res	MS Resolution	-	0.250	Rectangular	0.144	∞
c_c	Combined Correction	-				
u_c	Combined Uncertainty			Normal	0.195	19
U	Expanded Uncertainty			Normal	0.418	
$RM = (2.71 \pm 0.42)mm$						

Table 5: Uncertainty associated with circularity deviation measurements using A2M8 in all 4 positions.

	Experiment 1	Experiment 2	Experiment 3	Experiment 4
u_{Rep}	0.132	0.013	0.149	0.046
u_{Res}	0.144	0.144	0.144	0.144
c_c	0	0	0	0
u_c	0.195	0.147	0.207	0.152
U	0.418	0.293	0.452	0.304
RM	$(2.71 \pm 0.42)mm$	$(3.73 \pm 0.29)mm$	$(7.96 \pm 0.45)mm$	$(20.90 \pm 0.30)mm$

As we can infer from Figures 8 (a, b), because of the high sensibility measuring time of flight, that kind of sensor is naturally noisy, and should be used carefully. Depending on the application, it's resolution is acceptable, as long as a 10x

better resolution reference system is used to confirm the quality and applicability (Knapp, 1970).

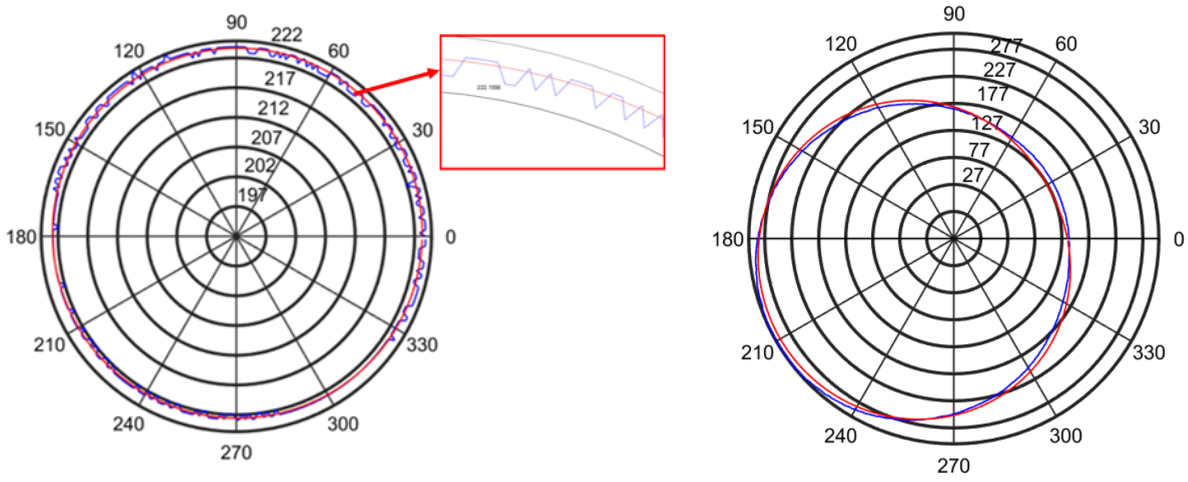

(a) Scan plot in MATLAB with the MS centralized. (b) Scan plot in MATLAB with the MS $85,755mm$ decentralized.

Figure 8: Measurements using $RPLiDAR\ A2M8$.

In Figure 9a, the circularity error obtained in our limaçon experiments is compared with the results obtained through the Gaussian best-fit method. As we can observe, in both approaches the smallest circularity error occurred in the position close to the center and the error increases according to the decentralization of the MS. In addition, the results indicate that the Gaussian method is less sensitive to the MS decentralization. The main hypothesis for this phenomenon is the error due to limaçon approximation (Figure 9b), which tends to zero when there is no eccentricity (see Eq. 7).

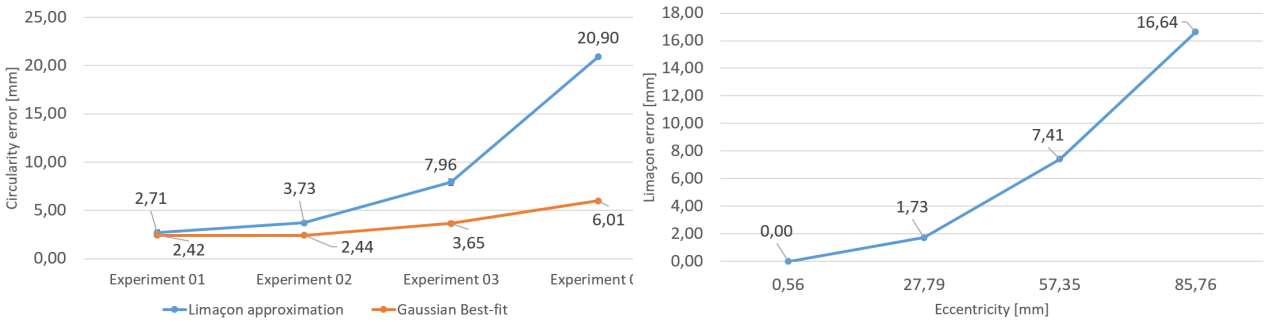

(a) Circularity error vs eccentricity. (b) Limaçon error vs eccentricity.

Figure 9: Measurements using $RPLiDAR\ A2M8$.

Samuel and Shunmugam (2003) observed that, as the MS is positioned further from the center of a coordinate system, the limaçon-shaped geometry will become increasingly distinct from a circle. In this context, Figure 2 illustrates that first the circle will get flattened on one side. As expected, Figure 10 shows that the maximum radius was not affected in our experiment. In contrast, the minimum radius decreases mainly due to the relation between the limaçon error and the MS eccentricity.

Figure 11 shows the effects of three angular velocities, $5,7\ Hz, 11,3\ Hz$ and $14.9\ Hz$, on the minimum radius, maximum radius and circularity error. In this experiment, each angular rate was tested five times, and the uncertainty associated with each rate was obtained using the same sources of uncertainty presented in Table (4). As Figure (11a) indicates, maximum and minimum radius are relatively insensitive to angular rate. In Figure (11b) we can observe that the lower the angular velocity of the LiDAR, the greater the circularity error due to a bigger point cloud measured in a single revolution at low speed, which results in more surface details.

As discussed in Section 3, the RM obtained in the experiments with the articulated 3D measuring arm was $0.889 \pm 0.078mm$. In contrast, the smallest RM obtained with the LiDAR and limaçon approximation was $2.71 \pm 0.42mm$ when the MS was in the highly centralized position and rotating at $11.3\ Hz$. The circularity error was substantially smaller in CMM measurements due to the system lower resolution compared to the RPLiDAR. The CMM also presents mechanical filters related to the probe and less points were evaluated on the process.

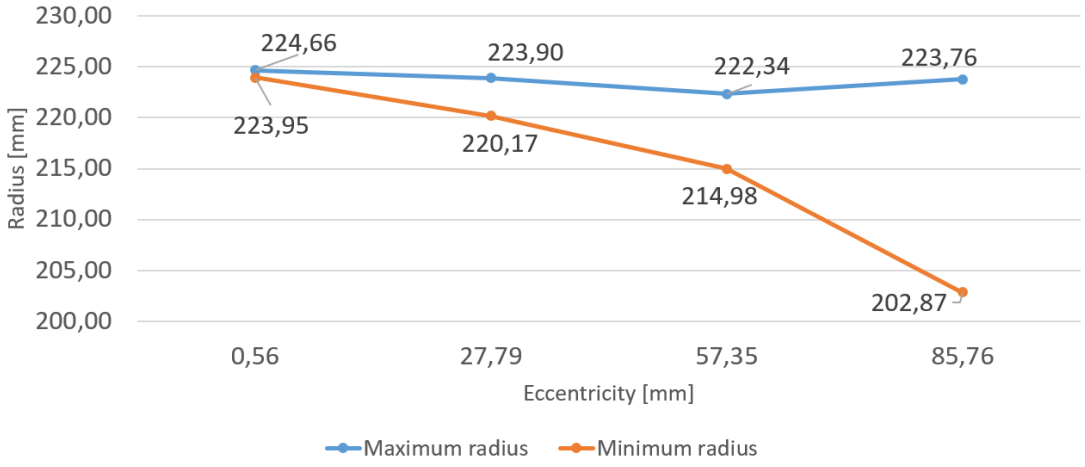

Figure 10: Radius vs eccentricity

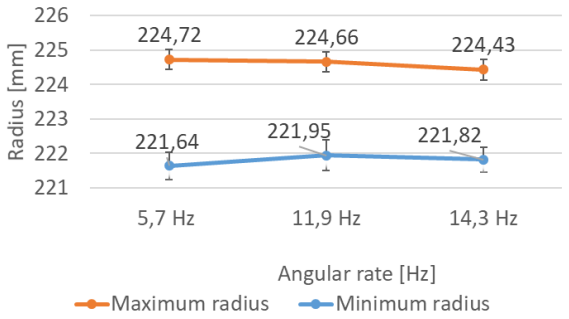

(a) Radius vs angular rate

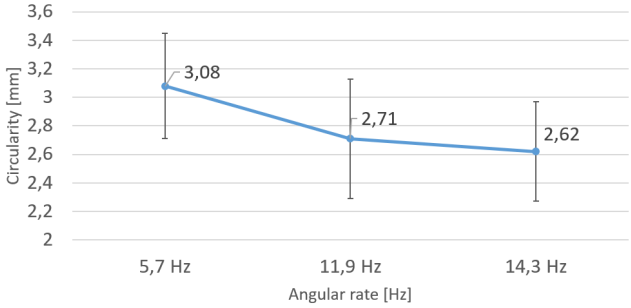

(b) Circularity error vs angular rate

Figure 11: Radius and circularity error in three angular rates: $5,7\ Hz$, $11,3\ Hz$ and $14.9\ Hz$.

5. CONCLUSIONS

This paper presented a research on the use of limaçon approximation and a LiDAR system to measure circularity. This approximation, which aims to represent the circle by a geometry called limaçon using polar coordinates, copes with drawbacks of best-fit techniques, such as iterative calculations. In the experiments, data points were captured in four positions, that is, one with the MS approximately concentric to the measurand, and the others with offsets. Next, the calculation of the circularity deviation by limaçon approximation and uncertainty measurement are performed to evaluate sources of uncertainty, such as resolution and Azimuth angle, and the effect of several parameters, namely angular rate, angular speed and number of revolutions, are evaluated. Finally, the results are compared with those obtained through an articulated 3D measuring arm, which is the reference system.

The results suggest limaçon approximation as a suitable technique to directly find the decentralization of a circularity MS. Moreover, even being a relatively cheap educational sensor, it is possible to use it as a practical tool to evaluate circularity error. As observed, the angle θ is incremented linearly, thus allowing the use of a linear equation to identify the unknown measurement parameters, making trivial the process of determining the center and radius of the measurand. The farther from the center the MS is, the bigger is the circularity error caused by the limaçon approximation. For this reason, this technique is not recommended for large eccentricities due to the non-circularity of the limaçon geometry. The circularity error was substantially smaller in the CMM measurements. Furthermore, ambient lighting may have contributed to differences between measurements with the LiDAR A2M8 and the CMM FARO. At lower angular speed, the circularity error was greater, and the main hypothesis is the bigger point cloud measured, which results in more surface details. Naturally, LiDAR systems carry high levels of noise, and better equipment will show a better resolution, therefore resulting in a model that better represents the characteristics of the measurand.

Next studies will aim to allow the limaçon approximation algorithm to employ the angles obtained in the measurement, not approximating them to the ideal θ. In addition, we aim to integrate the MS to a third axis of motion, enabling the capture of three-dimensional point clouds.

6. ACKNOWLEDGEMENTS

We would like to show our gratitude to the Federal University of Santa Catarina (UFSC), LABMETRO and CERTI Foundation.

7. REFERENCES

Adegboye, M.A., Fung, W.K. and Karnik, A., 2019. "Recent advances in pipeline monitoring and oil leakage detection technologies: Principles and approaches". *Sensors*, Vol. 19, No. 11, p. 2548.

Anton, H., Bivens, I. and Davis, S., 2014. *Cálculo - Volume II - 10° Edição*. Editora Bookman.

Chetwynd, D., 1979. "Roundness measurement using limaçons". *Precision Engineering*, Vol. 1, No. 3, pp. 137–141.

Chetwynd, D. and Phillipson, P., 1980. "An investigation of reference criteria used in roundness measurement". *Journal of Physics E: Scientific Instruments*, Vol. 13, pp. 530–538.

Costa, V., Haselein, B., Veras, F., Dutra, M. and Pinto, T., 2021. "Cob-2021-0943-repository". `https://github.com/vini-cc/COB-2021-0943-repository`.

Eves, H., 1965. *A Survey of Geometry Volume Two*. Allyn and Bacon.

Faro, 2016. *FARO Edge and FARO Laser ScanArmEdge Manual*. FARO Technologies, Inc., 250 Technology Park Lake Mary, FL 32746, EUA, 3rd edition. User Manual available at `https://knowledge.faro.com/Hardware/FaroArm_and_ScanArm`.

Hredil, M., Krechkovska, H., Student, O. and Kurnat, I., 2019. "Fractographic features of long term operated gas pipeline steels fracture under impact loading". *Procedia Structural Integrity*, Vol. 21, pp. 166–172.

Knapp, W., 1970. "Tolerance and uncertainty". *WIT Transactions on Engineering Sciences*, Vol. 34.

Movimed, 2018. "Laser triangulation". `https://www.movimed.com/knowledgebase/what-is-laser-triangulation/`. Accessed: 2021-06-02.

Muralikrishnan, B. and Raja, J., 2008. *Computational surface and roundness metrology*. Springer Science & Business Media.

Poldrack, R.A., 2019. *Statistical Thinking for the 21st Century*.

Samuel, G. and Shunmugam, M., 2003. "Evaluation of circularity and sphericity from coordinate measurement data". *Journal of Materials Processing Technology*, Vol. 139, No. 1-3, pp. 90–95.

Slamtec, 2017. *RPLiDAR A2*. Shanghai Slamtec Co, 2F, Building E, Shengyin Tower, 666 Shengxia Rd., Shanghai, China, 3rd edition. User Manual.

Souza, C.C., Arencibia, R.V., Costa, H.L. and Piratelli Filho, A., 2012. "A contribution to the measurement of circularity and cylindricity deviations". In *ABCM symposium series in Mechatronics*. Vol. 5, p. 791.

Sun, Q., Chen, J. and Li, C., 2015. "A robust method to extract a laser stripe centre based on grey level moment". *Optics and Lasers in Engineering*, Vol. 67, pp. 122–127.

8. RESPONSIBILITY NOTICE

The authors are solely responsible for the printed material included in this paper.